Installation and efficiency of the new 40 m radio telescope vertex membrane

P. de Vicente, F. Tercero, T. Finn
J.A. Abad, J. Fernández, J.M. Yagüe

Informe Técnico IT-OAN 2011-4

Revision history

Version	Date	Author	Updates
1.0	19-04-2011	P. de Vicente	First version
2.0	27-05-2011	T. Finn & F. Tercero	Rewritten and added many details on the installation of the membrane

Contents

1 Introduction

The membrane at the vertex of the 40 m radiotelescope has been replaced by a new one with less losses. This report offers a summary of the design of the new membrane, the installation in the telescope and the measurements performed using astronomical observations.

2 The vertex membrane

The 40 m radiotelescope has a membrane in the central tube that connects the vertex of the main reflector and the receiver cabin. The vertex of the main reflector is covered by a circular structure with eight petals that form a diaphragm. The petals are opened during observations and are closed during periods of inactivity thereby protecting the tube from the exterior weather conditions. Immediately after the actuators, that move the petals, there is a narrow steel ring mounted on the walls of the tube and perpendicular to its axis (figure 1). The surface forms an angle of 65 degrees with the axis tube, parallel to the path of the rays from the subreflector towards M3 (Fig. 1).

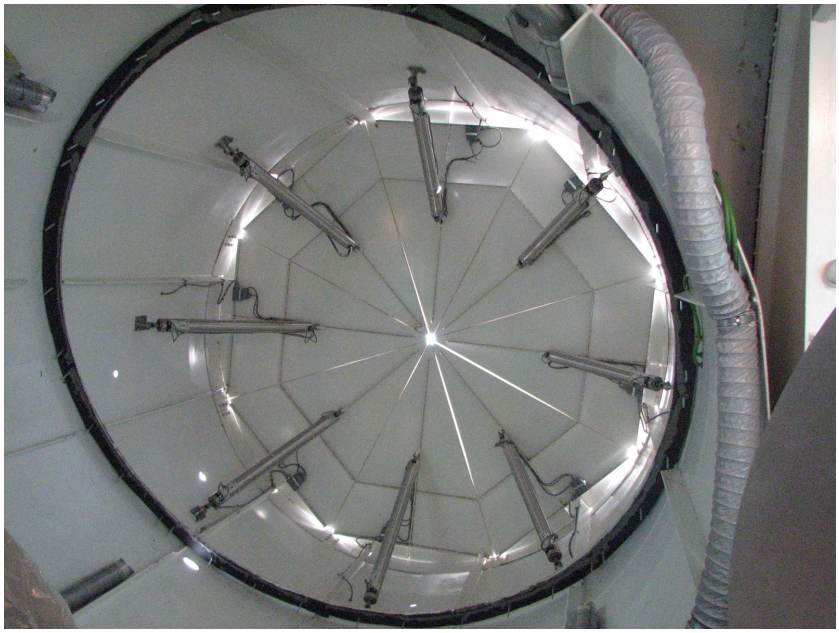

Figure 1: *The interior of the central tube.*

The vertex membrane lies against the ring and is held in place by a clamping system that also prevents water from the exterior entering the receiver cabin. Its shape is an elliposoid, obtained by cutting a cylinder with a plane with a tilt of 25 degrees with the cylinder axis. The major and minor axes have dimensions of 3.36 m and 3.05 m respectively.

The original membrane was made of plastic fabric about 0.4 mm thick. The membrane was mechanically resistant and waterproof. However if offered an impermeable surface which, while desirable to ensure a watertight environment, also suffered high levels of wind resistance.

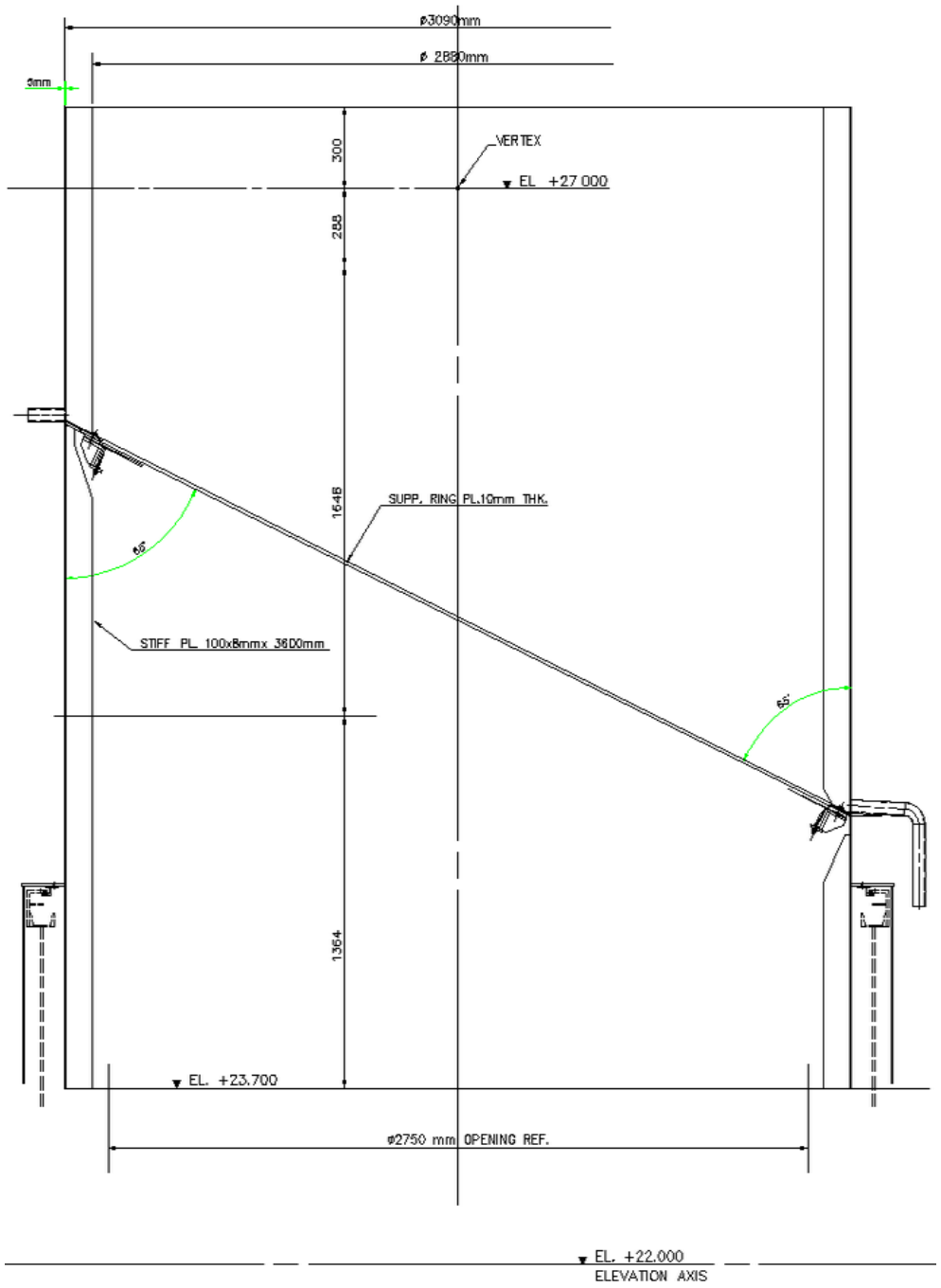

Figure 2: *Section of the tube showing the rim and the place where the mebrane is placed. The drain hole is connected to a J shape tube, which can be seen in the sketch.*

As a result, the old membrane had to be stretched taut. Nevertheless the surface slackened slightly and it tends to oscillate in the wind.

The membrane was clamped to the steel ring via 10 stainless steel pieces (Fig. 3) with the form of circular arcs which are heavy and difficult to manage. The entire border was then sealed with a silicon gel.

Figure 3: *Picture of the old membrane with the heavy iron support structures forming a circumference.*

Malo 2010 measured the dielectric constant and loss tangent of the membrane material and simulated, based on these values, the return losses via a simple impedance model under normal incidence. It demonstrates a maximum in reflection at 100 GHz of the order of 1.2 dB (25%).

Finn & Tercero (2011) have measured the free space losses as a function of angle of incidence and for the two orthogonal linear polarization vectors. These results are directly comparable to the in situ return losses that will be suffered by the membrane in the antenna vertex. The measured losses were found to be 1.4 dB for the parallel polarisation and 2.5 dB for the perpendicular polarisation which corresponds to losses of 28% and 44% respectively. The losses will depend not only on the mode of observation (i.e circular or linear receiver polarisation) but also on the polarisation of the astronomical source and the elevation angle of the telescope. Thus the mean loss for beam from an unpolarised source is 35%

3 New membrane

Since the membrane was rather inefficient at 3 mm, Finn & Tercero (2011) investigated materials for a new membrane. The tilting of the membrane to 25 degrees causes the perpendicular and parallel polarizations to have different transmission coefficients. This effect is particularly pronounced in high permittivity materials and thus the choice of an adequate material was focused on very low permittivity materials such as expanded and extruded polystyrene and polyethylene foams where the effective permittivity was very close to 1.

All materials tested had a very low permittivity and the final choice was based on practical issue. Polystyrene materials are very light and durable, where as the polyethylene foams are slightly denser and can be degraded by the UV. However, the polyethylene is very hand formable and elastic and recovers its shape after deformation and as a result exhibits better mechanical resistance than the more rigid polystyrene foam. Since the membrane is only exposed to UV radiation during short periods of time and tend to suffer more constantly from mechanical stress due to wind the polyethylene foam is preferred. Additionally the flexibility of the foam greatly enhances the ease of installation by allowing the deformation of the ellipsoidal surface to the actual shape of the central tube. Further details relating to the physical characteristics of the PE foam may be found in the Annex II.

The new membrane was purchased by the end of 2010. It is made of Polyethylene foam and has a thickness of 53 mm. The manufacturer only offers various thicknesses and 53 mm was considered sufficient to guarantee the structural integrity of the new membrane. The dimensions are 3.36 m for the major axis and 3.05 m for the minor axis. The membrane was requested in a single piece but the manufacturer delivered an ellipsoid made of 6 parts formed from a zigzag cut assembled with glue.

In order to install the new membrane a new set of metallic supports were designed and constructed from aluminium. Figure 4 below displays the original design for the PE membrane including the aluminium supports.

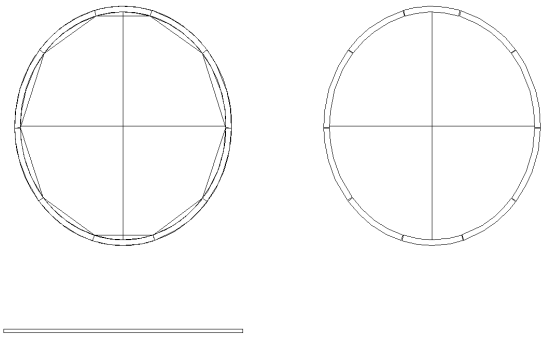

Figure 4: *The new membrane and its metal supports.*

4 Membrane installation

The membrane was replaced in two stages taking advantage of a period of 10 days with good, dry weather. The old membrane was removed on April 11th. The first installation day was quite windy requiring the antenna to be turned offering the back-structure to the wind. A wind of 40 km/h is rather inconvenient if the antenna points towards it. In order to remove the membrane the antenna was tilted to 5 degrees elevation, allowing the workshop personnel to enter the tube from the receiver cabin.

4.1 Membrane Removal

The old membrane and supports were removed with prior numbering of each one. Once the membrane was removed, the rim was cleaned of silicon traces. The operation took 4 hours approximately. When the old membrane was removed it was observed that the screws had damaged the membrane where they made contact due to wear and tear.

4.2 Membrane Installation

The installation consisted of three stage

1. The preparation of the membrane for installation in an appropriate area (e.g hangar building)
2. The transport of the membrane to the receiver cabin
3. The installation of the membrane within the vertex

Each stage consisted of one or more procedures which are described below

4.3 Membrane preparation

- The metallic supports were constructed after in situ measurement of the membrane in the vertex (see ACAD drawings Annex I)
- The joints were then sealed on the exterior face (face oriented towards sub-reflector) using a polyurethane gel due to several demonstrating a lack of water tightness (24 hr curing, for additional information see Annex III)
- The old steel supports and membrane were mounted on top of the new membrane to define the location of the drill holes and to permit the approximate centring of the border of the membrane. The excess sections were then removed with a Stanley blade.
- The headless bolts used for the installation are M8 and 100 mm in length and were mounted in their corresponding holes in the antenna vertex (figure 6). The original bolts were insufficiently long to accommodate the new membrane.

- The new membrane was drilled with 40 holes with each one containing a metallic cylinder 15 mm diameter which protect the foam from general abrasion by the bolts. They also permit a degree of lateral freedom when mounting the membrane in the vertex.
- A second spare membraneis dimensions and drill holes was marked via the first membrane.

Figure 5: *The mounting bolts on the steel ring.*

4.4 Transport

- The membrane was placed horizontally on the scissor platform and raised to the receiver cabin balcony.
- The membrane was then introduced to the cabins interior and laid on the floor on level 19 metres. The membrane is quite flexible and was manipulated and bent with care in order to pass the K and W band receivers.

4.5 Installation

- The metallic barrier on level 20.7 meters was removed for ease of access.
- M3 was rotated through 90 degrees
- The membrane was lifted manually and introduced by translation and rotation into the telescope vertex with the watertight face towards the subreflector. A first coat of Polyurethane gel is applied to the steel ring before the installation of the membrane.

Figure 6: *The new membrane was lifted on the telescopic platform and taken inside the receiver cabin.*

- Since the membrane is virtually the exact same size and the placement was impeded by the axial tube re-enforcements the bottom part had to be introduced first. It was also necessary to have a technician on the far side of the membrane to guide the interior installers.
- The first four headless bolts were introduced to their respective drill holes. However it was necessary to deform the membrane somewhat to achieve this goal.
- Once these first bolts had been successfully engaged the remaining 36 bolts entered their respective drill holes with relative ease (Fig. 7)
- Once all bolts are in place the metallic supports were mounted in quadrants while a technician injected a polyurethane gel on the exterior joint between the membrane and the steel ring.

The membrane was then subjected to water tightness testing which showed leaks. These were filled in over a period of a week by pouring water on the membrane from the exterior and during a period of intense rain the weekend following the installation.

Finally, figure 8 displays the new membrane after installation and indicates the relation between the orientation of the membrane and mounting plate with respect to the sequential numbering of the joints.

5 Astronomic measurements at 86 GHz

In order to characterize the new membrane, observations of Venus and Saturn at 86 GHz were performed two days before removing the old membrane, without membrane and after placing

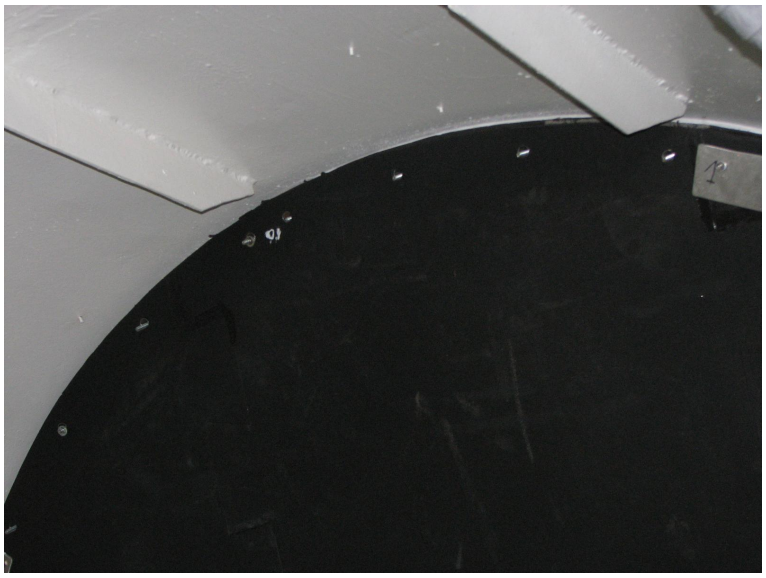

Figure 7: *The membrane after bolt penetration of all drill holes. The first mounting plate can be seen.*

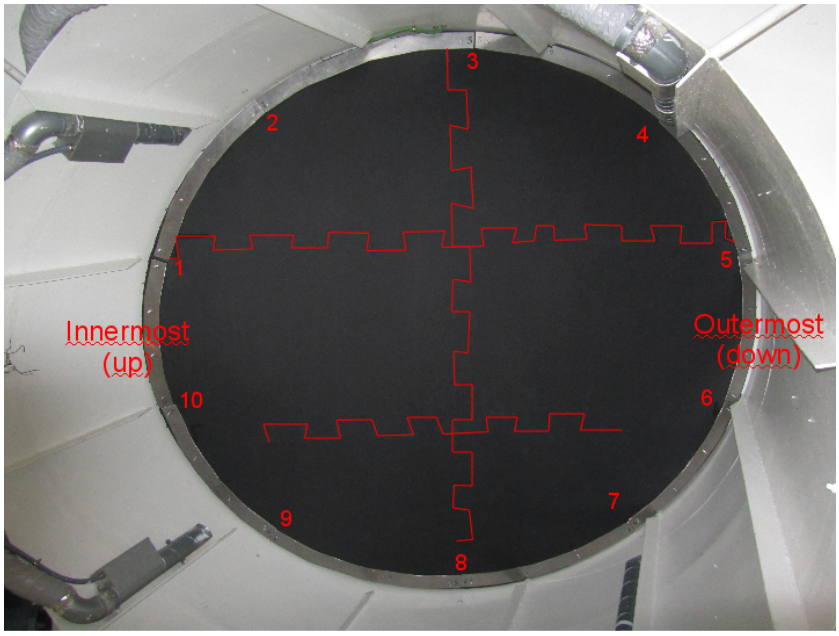

Figure 8: *Picture of the new membrane from the receiver cabin. The zizag cut between the differente pieces has been highlighted in red. The interface between the new supports is also tagged in red.*

the new one. Unfortunately we found some problems with the mm receiver during the first days that prevented having good measurements of Venus. Results are summarized in table 1

The aperture efficiency (η_a) of the antenna depends on several factors: the efficiency of the main reflector (η_{m1}), subreflector (η_{m2}) and all other mirrors (η_{nm}). These arise from surface errors and can be estimated from the Ruze formula and assuming a given surface RMS error. The membrane efficiency (η_{mb}) also affects the overall efficiency as well as blockage by the legs and subreflector (η_b), and illumination (η_i).

$$\begin{aligned} \eta_a &= \eta_{m1}\eta_{m2}\eta_{nm}\eta_{block}\eta_{mb}\eta_i & (1)\\ &= \eta_{m1}\eta_{m2}\eta_{m3}\eta_{m4}\eta_{m22}\eta_{block}\eta_{mb}\eta_i & (2)\end{aligned}$$

where we have ignored the errors coming from all mirrors after M22.

According to Ruze (1966) the estimated efficiency obtained from the rms of the surface:

$$\eta_{mirror} = e^{-\frac{4\pi\sigma}{\lambda}^2} \tag{3}$$

where $\lambda = 3.3$ mm at 86 GHz and σ is 50 μm for the subreflector, 25 μm for M3 and M4 and 40 μm for M22.

The efficiency due to blockage is 0.92 (de Vicente 1998), and the efficiency due to illumination 0.7 (Tercero private communication).

Hence at 3 mm:

$$\eta_a = \eta_{m1}\, 0.967\, 0.99\, 0.99\, 0.98\, 0.92\, \eta_{mb}\, 0.7 = 0.60\, \eta_{m1}\, \eta_{mb} \tag{4}$$

The aperture efficiency can be estimated from pointing drifts towards planets, whose brightness can be approximated by a black body. According to Baars (2007):

$$\eta_a = \frac{2K_B C_s T'_a}{AS_f} \tag{5}$$

where T'_a is the antenna temperature corrected by the atmospheric attenuation, A the radiotelescope collecting area, S_f the source flux and C_s a factor which takes into account the source brightness distribution compared to the antenna HPBW and is only valid for sources whose size is equal or smaller than the beam width:

$$C_s = \begin{cases} 1 + x^2 & \text{gaussian source} \\ \frac{x^2}{1-\exp(-x^2)} & \text{disk source} \end{cases} \tag{6}$$

where,

$$x = \frac{\theta_s('')}{\theta_b('')} \tag{7}$$

and θ_s is the source size and θ_b the HPBW of the antenna.

For the 40 m radiotelescope we can simplify:

$$\eta_a = 2.196 \frac{C_s\, T'_a[\mathrm{K}]}{S_f[\mathrm{Jy}]} \tag{8}$$

Results are summarized in table 1. Observations of Saturn were performed during the night and since the atmosphere was more stable and the tetrapod legs do not expand due to the action of the sun, they have a better quality than Venus observations. Venus observations were done during the day. The planet preceeded the Sun by 2 hours at an angular distance of 30 degrees approximately. The subreflector and the tetrapod legs were illuminated by the sun. This affected the focus, which differed -2 mm along the Z axis with respect to the night. The other subreflector axis were also affected. All these circumstances caused the observations to have worse quality than observations of Saturn. The best moment to observe Venus was early in the morning.

Membrane	Source	Size (")	Flux (Jy)	C_s	T'$_a$ (K)	S/T'$_a$ (Jy/K)	η_a
Old (1)	Venus	$12.5'' \times 12.5''$	245	1.18	> 5.4	< 58	> 0.057
None (1)	Venus	$12.5'' \times 12.5''$	235	1.18	> 9.5	< 33	> 0.065
New	Venus	$12.5'' \times 12.5''$	235	1.18	11.3± 1	17± 20	0.124 ± 0.008
Old	Saturn	$19'' \times 17''$	203	1.39	6.2± 0.5	25± 10	0.093 ± 0.004
None	Saturn	$19'' \times 17''$	203	1.39	10.2± 0.5	14± 10	0.153 ± 0.004
New	Saturn	$19'' \times 17''$	203	1.39	8.5± 0.5	17± 10	0.128 ± 0.004

Table 1: *Size, flux, antenna temperature (corrected by opacity), source correction, flux antenna temperature ratio and aperture efficiency for Venus and Saturn at 86.2 GHz. All data were taken at 30 degrees elevation approximately. HPBW at 86.2 GHz is* $18''$*. (1) These observations were of very poor quality and should be taken with care.*

As we can see from table 1 the antenna aperture efficiency is 15.3% without membrane, 12.6% with the new membrane, and 9.3% with the old membrane. These values, however require a correction that we exaplin in next subsection.

5.1 Linearity of the 3 mm IF continuum detectors

We have investigated the linearity of the measurements at 3 mm and have found that up to April 25th 2011, continuum measurements obtained with the Pocket Backend and using an IF attenuation of 8 dB were not linear. Since the IF signal feeds the VLBA terminal we found that when inserting the hot load, the VLBA square detectors saturated and the maximum volt obtained was 5.53 V. We tried again with an IF attenuation of 10 dB and all measurements, including the most extreme ones (hot and cold load), were in the linear regime of the VLBA square law detector (except for the zero). We have checked the difference in the estimation of the receiver temperature in both cases and, in the non-linear regime, the receiver temperature was 97 K versus 79 K in the linear regime. We have also performed some pointing drifts towards Venus in both cases and found that the antenna temperature is 1.19 times higher in the non-linear regime than in the linear one. Therefore all parameters derived from antenna temperature should be corrected by this factor.

Taking into account a correction of 1.19, the antenna aperture efficiencies that we determine in the three cases are summarized in table 3:

Attenuation (dB)	Hot Load (V)	Cold Load (V)	Sky (V)	Zero (V)	T_r (K)
8	5.53	1.58	2.82	0.02	97
10	4.18	1.09	1.78	0.02	79

Table 2: *Voltages in a calibration scan with two different attenuation IF values for the 3 mm receiver. The maximum value given by the square detector is 5.53 Volts, hence the detector was saturated when the receiver was seeing the hot load. The receiver temperature is in the last column. The correct value is the one in the second line.*

Membrane	Efficiency	η_a
Old	0.61	7.9%
New	0.82	10.9%
None	1.0	13.2%

Table 3: *Membrane efficiency and antenna aperture efficiency with two types of membranes at the vertex and no membrane.*

The efficiency of the main reflector can be obtained from the aperture efficency when there is no membrane at the vertex:

$$\eta_{m1} = \frac{\eta_a}{0.60} = 0.22 \tag{9}$$

and we can now estimate the surface error budget for M1 using Ruze formula:

$$\sigma = \frac{\sqrt{-\ln \eta_{m1}}}{4\pi} \lambda \, [\mu\mathrm{m}] \tag{10}$$

$$\sim 347 \, \mu\mathrm{m} \tag{11}$$

This value is in the same range as the one estimated from holographic measurements by J.A. López Pérez (Private communication).

Fig. 9 shows three continuum drifts towards Saturn with the old membrane, the new mebrane and no membrane at the vertex.

6 Checking the membrane losses

In order to check the losses introduced by the new membrane we inserted a small piece of the material of which the new membrane is made of, in the trajectory of the 3 mm beam and compared the results with similar observations without that material. Observations were done towards Venus. The atmosphere was quite good although not totally perfect and this may influence the results. The antenna temperatures were obtained after correcting for pointing and focusing and after slewing from a position in which the sun did not illuminate directly neither the tetrapod legs nor the subreflector. The pointing error was in all cases below 2 arcsecs.

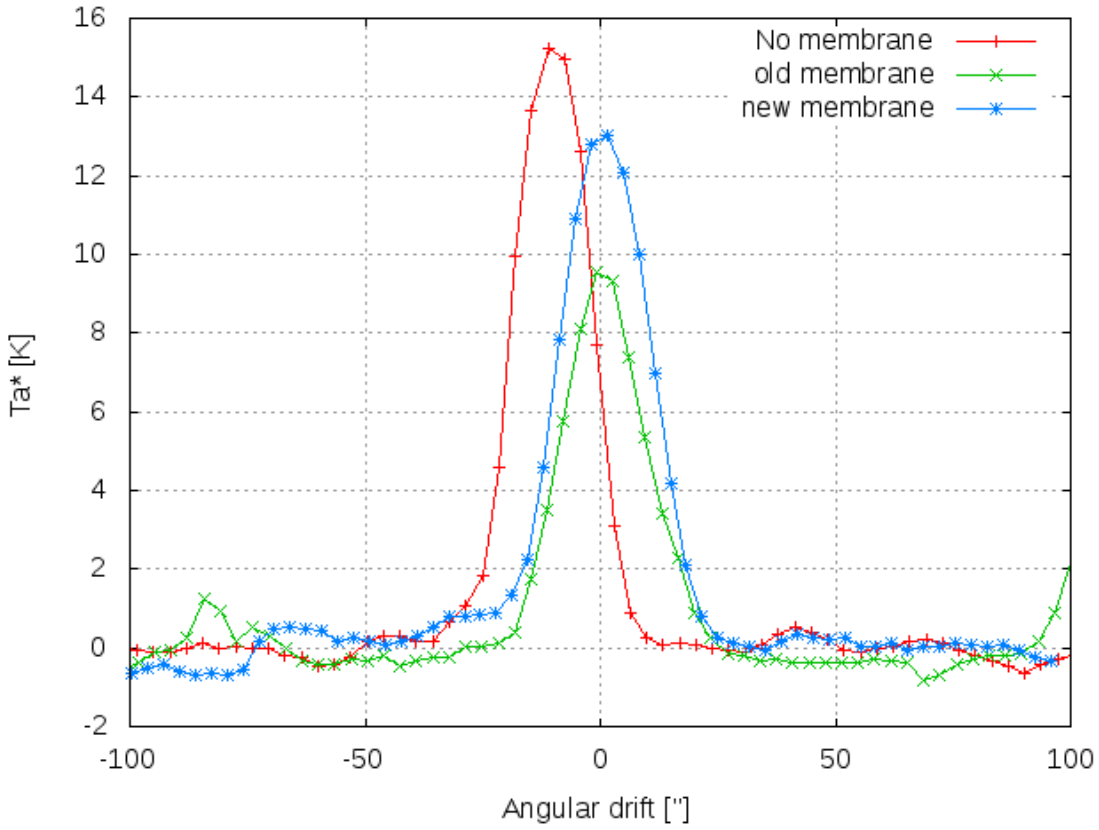

Figure 9: *Pointing drifts towards Saturn with the old membrane, no membrane and the new membrane. All were done at 30 degrees elevation at 86.24 GHz. Intensity scale is Ta**

The membrane was placed besides the fist 3 mm mirror and formed an angle of approximately 45 degrees with the beam. Since this mirror is after the hot load, we calibrated the observation without any obstacle in front of the mirror and did not repeat it while the piece of material was being used. In this way we avoided altering the calibration by placing the material in front of the hot load. The placement of the material in this position may have not been the best since the ray crosses the material twice (see Fig. 10)

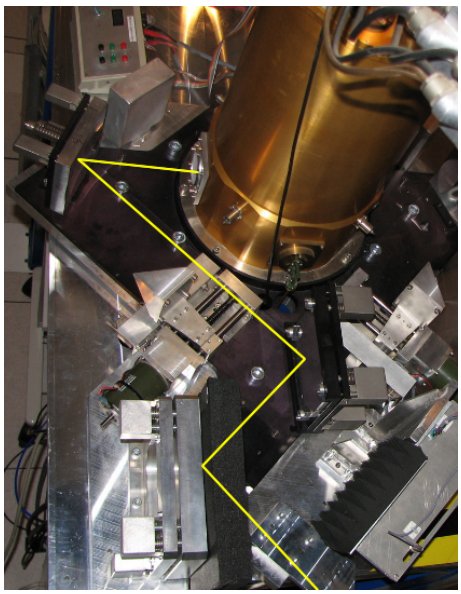

Figure 10: *Mirrors before the 3 mm. The yellow line shows the path of the rays reflecting on 3 mirrors. The rays first reflects on the mirror, in front of which a piece of material like the membrane was placed. This picture shows the corner cube in the trajectory, and the hot load out of the trajectory. At this position the cryostat is looking at the cold load inside itself.*

The mean antenna temperature (T_a^*) towards Venus with the small piece of membrane in front of the horn was 11.6 K and 12.7 K, without it. This difference implies that the new membrane has an efficiency of 0.95 and losses are approximately 5%, where we have taken into account that radiation crosses twice the test membrane. On the other hand the system temperature increases from 165±4 K to 179±4 K without and with the membrane of new material respectively. If the membrane has dissipative losses this increase may come from them. Taking into account that 0.1 dB loss at ambient temperarure generates 7 K in excess in system temperature, the total dissipative losses are 0.2 dB (5%) which corresponds to an efficiency of 0.95 for the new membrane. Results are summarized in table **??**

7 Skydips

We did two skydips on the same day without membrane and with the new membrane at the vertex. The first skydip was observed at 09:00 local time and the second one at 15:30. The water content at both times was different and hence opacity is also different. Fig. 11 shows the

Piece	T'_a(K)	Loss fraction	$T_{\rm sys}$(K)	Loss fraction
Inserted	11.6	9%/2	179	5%
None	12.7		165	

Table 4: *Antenna temperature and system temperature towards Venus with and without a piece of PTE foam (the same material and thickness of the vertex membrane), in front of mirror before the 3 mm receiver. The piece is seen in picture 10. The loss in the third column is obtained from the ratio of antenna temperatures. The loss in the fifth column is obtained from the increase in the system temperature.*

data and two fits per curve. The fits were done by hand and are depicted to show the range in which the forward efficiency and the opacity range.

The skydip without membrane, requires a zenital opacity between 0.20 and 0.22 and a forward efficiency between 0.71 and 0.73. The estimated opacity towards the zenith by ATM from surface parameters is 0.17, which apparently subestimates the opacity derived from the skydip. The skydip with the new membrane requires a zenital opacity between 0.18 and 0.20 and a forward efficiency between 0.66 and 0.68. The estimated opacity from ATM and using surface weather parameters is 0.155 which, as in the previous case, is a lower value than that obtained from the skydip.

The difference in opacity matches that from the different weather conditions. The difference in the forward efficiency is a way to describe that power from the sky is higher when the new membrane is in its place than when there is no membrane. This difference is:

$$\Delta T = T_{amb1}\,\eta_{f1} - T_{amb2}\,\eta_{f2} = 283\,\cdot 0.72 - 296\,\cdot 0.67 = 5.5\,K \tag{12}$$

This means that the new membrane would generate an extra noise of 5 K.

8 Gain as function of elevation

The increase in appearture efficiency has allowed to measure the gain of the antenna as a function of elevation using quasars. We have measured it by making total power drifts towards Saturn, 3C454.4 and 3C84 during a very clear day without clouds. The drifts required continuous pointing corrections. It is the first time that two quasars are detected at 3 mm using continuum drifts. The results are in Fig. 12. This curve should be repeated with a better pointing model.

9 Cleaning M3

Nasmyth mirror M3 was cleaned from dust and grease stains using some cloths wet with water. The cloths were not wiped along the surface to avoid scratches that may damage the mirror.

10 Conclusion

The old membrane had big losses at 3 mm, and once replaced by the new one, the efficiency has increased 35%. The current estimation for the aperture efficiency with the new membrane

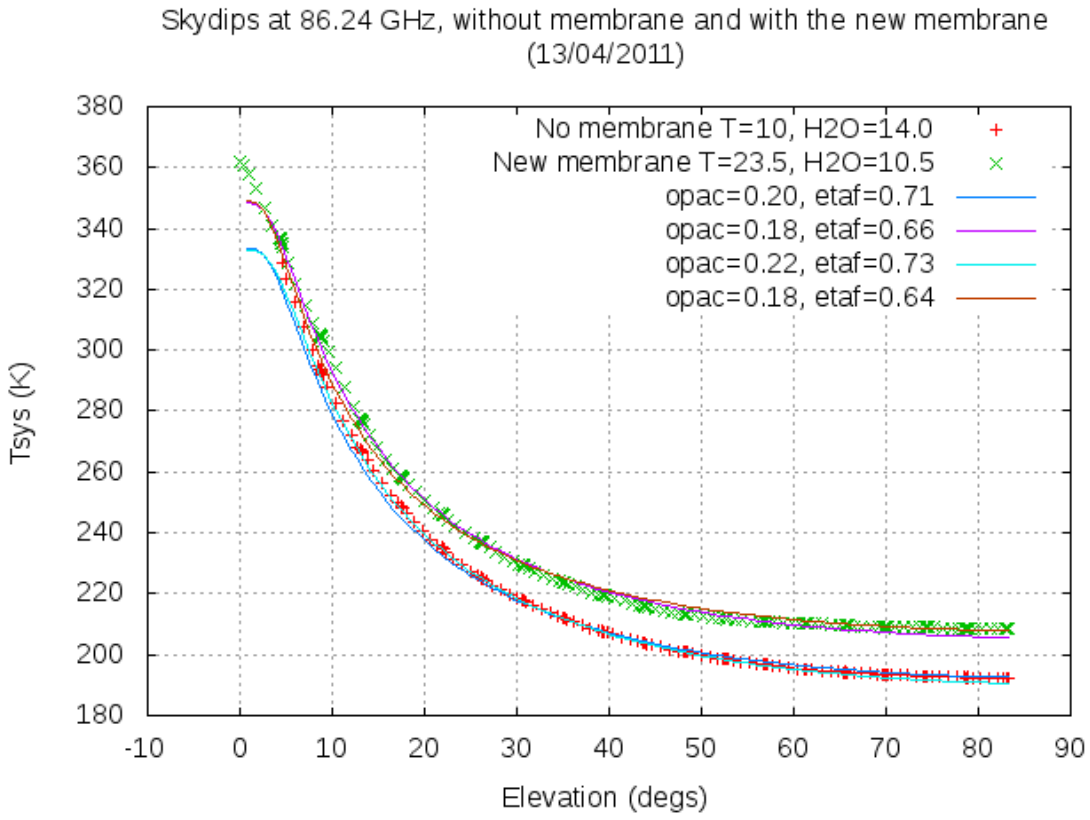

Figure 11: *Skydips without the membrane and with the new membrane at the vertex. Forward efficiency is 0.72 without membrane and 0.67 with the new membrane.*

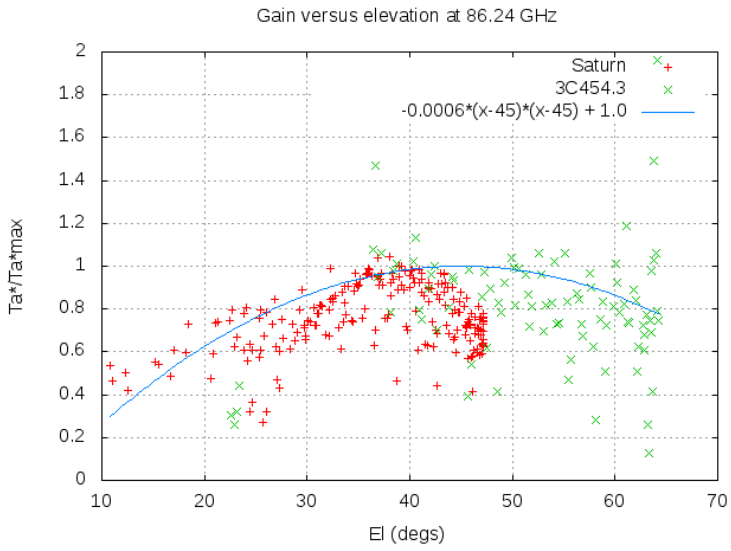

Figure 12: *Gain versus elevation from drifts towards Saturn and 3C454.3. The antenna temperature has been normalized.*

is 10.9%. We have tried to estimate the efficiency of the new membrane and find discrepant values. Direct measurements account for an efficiency of 0.82 which implies losses of 18%. Measurements from skydips and inserting a membrane of the same matreial and thickness in the ray path indicate an efficiency of 0.95 and losses of 5%.

The RMS error surface for the main reflector was estimated when no membrane was at the vertex and it is 347 μm at the time of this report.

References

[de Vicente 1998] P. de Vicente "Eficiencia por bloqueo en un paraboloide". IT–OAN 1998/10, 2010.

[Malo et al. 2010] I. Malo, J. D. Gallego, M. Diez, I. López, R. García. "Medida de la Permitividad a temperaturas criogénica y ambiente con el método de Perturbación de Cavidad". IT–OAN 2010/09, 2010.

[Finn and Tercero 2011] F. tercero, T. Finn, In preparation, 2011.

11 Annex 1. AutoCAD drawings of membrane and supports

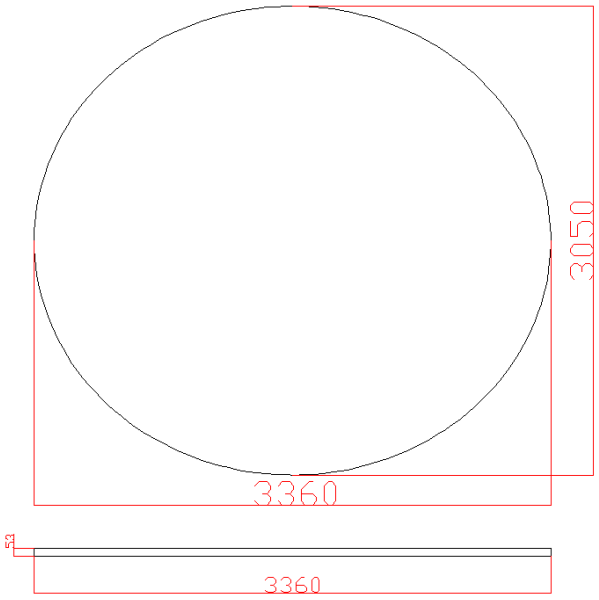

Figure 13: *Soportes_Espuma.dwg file contain the drawings of the supports.*

12 Annex II. PE foam technical datasheet

TECH FOAM

TECHNICAL FOAM, S.L.

HOJA TÉCNICA

Telf. 93 771 49 21
Fax. 93 771 47 82
Aptdo. Correos 251
08760 Martorell
Barcelona (Spain)

Espumas Técnicas y Autoadhesivos

PoliTec TA 33

Espuma de Polietileno físicamente reticulado

PROPIEDADES	NORMA	UNIDADES	VALORES
Densidad	ISO 845	Kg. /m³.	33 ± 3.5
Resistencia a la Tracción :			
(Longitudinal)	ISO 1926	KPa.	400 ⊥ 4%
(Transversal)	ISO 1926	KPa.	265 ± 4%
Alargamiento : (Longitudinal)	ISO 1926	%	130 ± 4%
(Transversal)	ISO 1926	%	125 ± 4%
Resistencia a la Compresión:			
Al 10%	ISO 844	KPa.	19
Al 25%	ISO 844	KPa.	40
Al 50%	ISO 844	KPa.	105
Deformación Remanente a Compresión Cte. :			
(22hr., 25%,23°C.)			
A los 30 min.	ISO 1856-C	%	20
A las 24h.	ISO 1856-C	%	10
Dureza		Shore "0" / "00"	17 / 50
Absorción agua tras 7 días		% Vol.	< 1
Rango de Temperaturas		°C.	- 80 / +100
Conductividad Térmica:			
A 10°C	ISO 2581	W/mK	0,034
A 40°C	ISO 2581	W/mK	0,039

Esta información es presumiblemente exacta y dada de buena fe. Los datos se basan en valores suministrados por nuestro proveedor y deben ser considerados solamente como directivas.

FichTec.doc 01-09-2005 Rev. 03

Figure 14:

13 Annex III. Polyurethane Sealant Datasheet

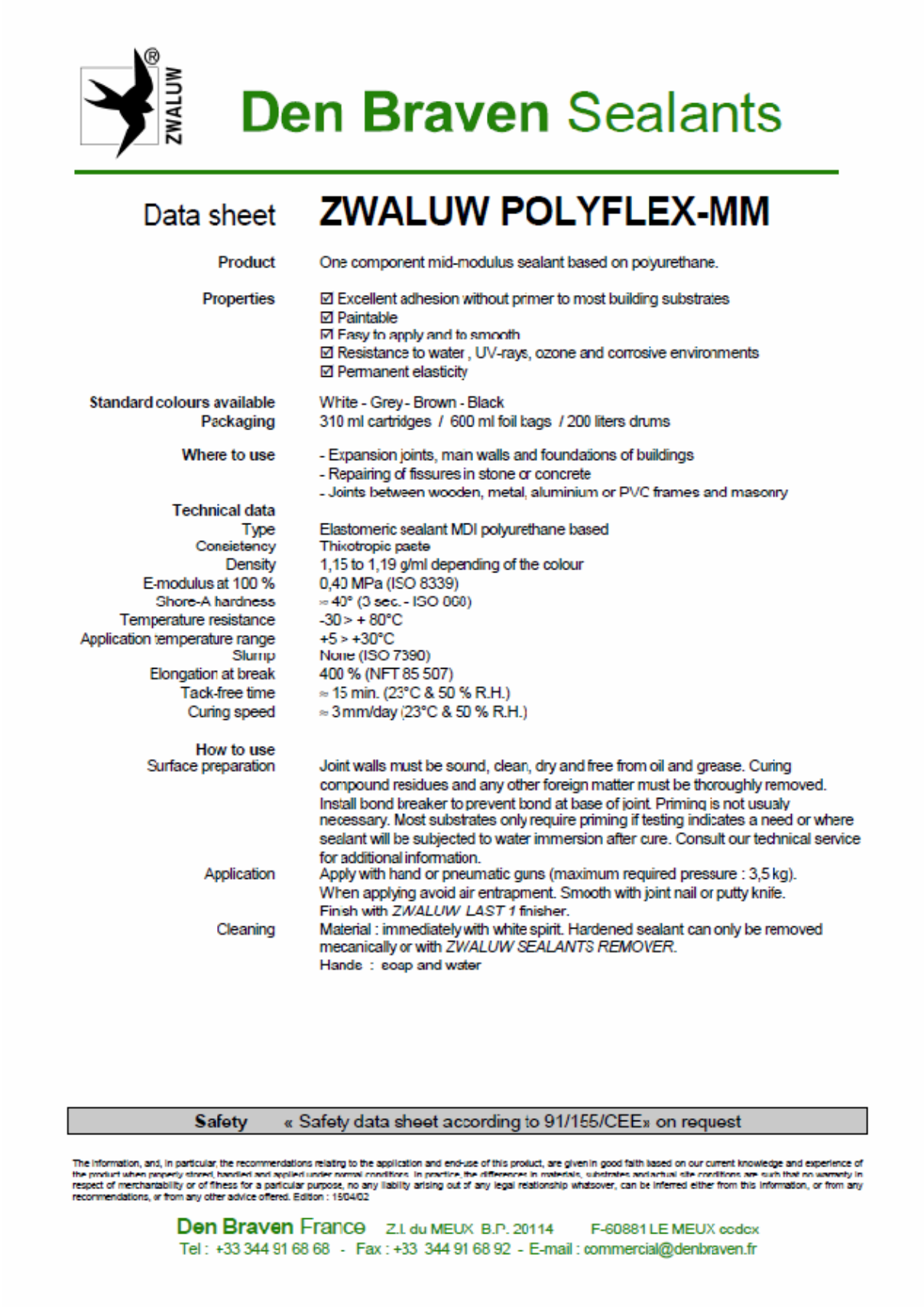

Den Braven Sealants

Data sheet **ZWALUW POLYFLEX-MM**

Product	One component mid-modulus sealant based on polyurethane.
Properties	☑ Excellent adhesion without primer to most building substrates ☑ Paintable ☑ Easy to apply and to smooth ☑ Resistance to water , UV-rays, ozone and corrosive environments ☑ Permanent elasticity
Standard colours available	White - Grey - Brown - Black
Packaging	310 ml cartridges / 600 ml foil bags / 200 liters drums
Where to use	- Expansion joints, main walls and foundations of buildings - Repairing of fissures in stone or concrete - Joints between wooden, metal, aluminium or PVC frames and masonry
Technical data	
Type	Elastomeric sealant MDI polyurethane based
Consistency	Thixotropic paste
Density	1,15 to 1,19 g/ml depending of the colour
E-modulus at 100 %	0,40 MPa (ISO 8339)
Shore-A hardness	≈ 40° (3 sec. - ISO 868)
Temperature resistance	-30 > + 80°C
Application temperature range	+5 > +30°C
Slump	None (ISO 7390)
Elongation at break	400 % (NFT 85 507)
Tack-free time	≈ 15 min. (23°C & 50 % R.H.)
Curing speed	≈ 3 mm/day (23°C & 50 % R.H.)
How to use	
Surface preparation	Joint walls must be sound, clean, dry and free from oil and grease. Curing compound residues and any other foreign matter must be thoroughly removed. Install bond breaker to prevent bond at base of joint. Priming is not usualy necessary. Most substrates only require priming if testing indicates a need or where sealant will be subjected to water immersion after cure. Consult our technical service for additional information.
Application	Apply with hand or pneumatic guns (maximum required pressure : 3,5 kg). When applying avoid air entrapment. Smooth with joint nail or putty knife. Finish with *ZWALUW LAST 1* finisher.
Cleaning	Material : immediately with white spirit. Hardened sealant can only be removed mecanically or with *ZWALUW SEALANTS REMOVER*. Hands : soap and water

Safety « Safety data sheet according to 91/155/CEE» on request

The information, and, in particular, the recommendations relating to the application and end-use of this product, are given in good faith based on our current knowledge and experience of the product when properly stored, handled and applied under normal conditions. In practice, the differences in materials, substrates and actual site conditions are such that no warranty in respect of merchantability or of fitness for a particular purpose, no any liability arising out of any legal relationship whatsoever, can be inferred either from this information, or from any recommendations, or from any other advice offered. Edition : 15/04/02

Den Braven France Z.I. du MEUX B.P. 20114 F-60881 LE MEUX cedex
Tel : +33 344 91 68 68 - Fax : +33 344 91 68 92 - E-mail : commercial@denbraven.fr

Figure 15:

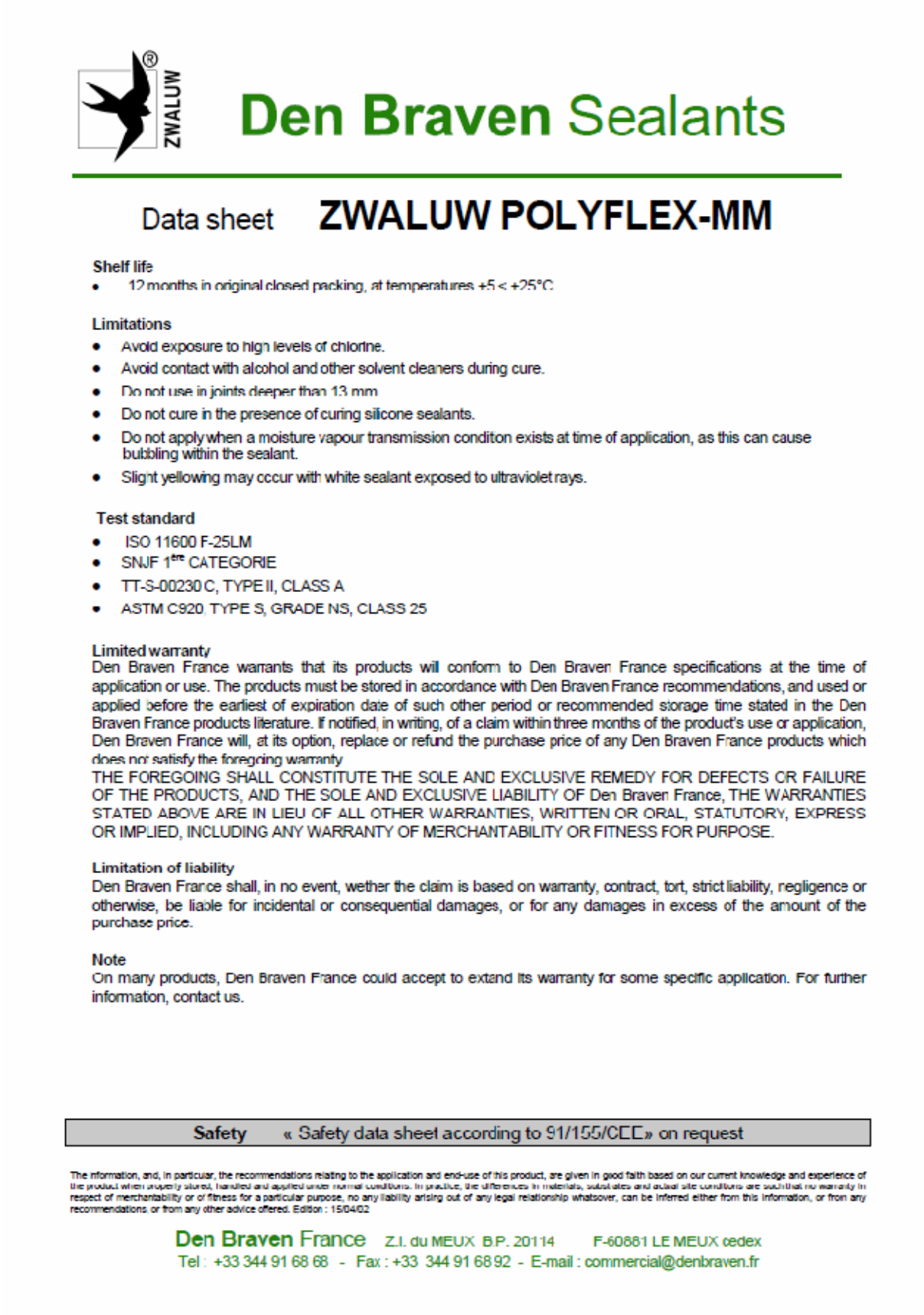

ZWALUW

Den Braven Sealants

Data sheet ZWALUW POLYFLEX-MM

Shelf life

- 12 months in original closed packing, at temperatures +5 < +25°C

Limitations

- Avoid exposure to high levels of chlorine.
- Avoid contact with alcohol and other solvent cleaners during cure.
- Do not use in joints deeper than 13 mm
- Do not cure in the presence of curing silicone sealants.
- Do not apply when a moisture vapour transmission conditon exists at time of application, as this can cause bubbling within the sealant.
- Slight yellowing may occur with white sealant exposed to ultraviolet rays.

Test standard

- ISO 11600 F-25LM
- SNJF 1ère CATEGORIE
- TT-S-00230 C, TYPE II, CLASS A
- ASTM C920 TYPE S, GRADE NS, CLASS 25

Limited warranty

Den Braven France warrants that its products will conform to Den Braven France specifications at the time of application or use. The products must be stored in accordance with Den Braven France recommendations, and used or applied before the earliest of expiration date of such other period or recommended storage time stated in the Den Braven France products literature. If notified, in writing, of a claim within three months of the product's use or application, Den Braven France will, at its option, replace or refund the purchase price of any Den Braven France products which does not satisfy the foregoing warranty

THE FOREGOING SHALL CONSTITUTE THE SOLE AND EXCLUSIVE REMEDY FOR DEFECTS OR FAILURE OF THE PRODUCTS, AND THE SOLE AND EXCLUSIVE LIABILITY OF Den Braven France, THE WARRANTIES STATED ABOVE ARE IN LIEU OF ALL OTHER WARRANTIES, WRITTEN OR ORAL, STATUTORY, EXPRESS OR IMPLIED, INCLUDING ANY WARRANTY OF MERCHANTABILITY OR FITNESS FOR PURPOSE.

Limitation of liability

Den Braven France shall, in no event, wether the claim is based on warranty, contract, tort, strict liability, negligence or otherwise, be liable for incidental or consequential damages, or for any damages in excess of the amount of the purchase price.

Note

On many products, Den Braven France could accept to extend its warranty for some specific application. For further information, contact us.

Safety « Safety data sheet according to 91/155/CEE» on request

The information, and, in particular, the recommendations relating to the application and end-use of this product, are given in good faith based on our current knowledge and experience of the product when properly stored, handled and applied under normal conditions. In practice, the differences in materials, substrates and actual site conditions are such that no warranty in respect of merchantability or of fitness for a particular purpose, no any liability arising out of any legal relationship whatsover, can be inferred either from this information, or from any recommendations or from any other advice offered. Edition : 15/04/02

Den Braven France Z.I. du MEUX B.P. 20114 F-60881 LE MEUX cedex
Tel : +33 344 91 68 68 - Fax : +33 344 91 68 92 - E-mail : commercial@denbraven.fr

Figure 16: